JOURNAL OF BACTERIOLOGY, Mar. 1995, p. 1444–1451 Vol. 177, No. 6
0021-9193/95/$04.00+0

The S-Layer from *Bacillus stearothermophilus* DSM 2358 Functions as an Adhesion Site for a High-Molecular-Weight Amylase

EVA EGELSEER, INGRID SCHOCHER, MARGIT SÁRA,* AND UWE B. SLEYTR

Zentrum für Ultrastrukturforschung and Ludwig Bolzmann-Institut für Molekulare Nanotechnologie, Universität für Bodenkultur, A-1180 Vienna, Austria

Received 23 September 1994/Accepted 30 December 1994

The S-layer lattice from *Bacillus stearothermophilus* DSM 2358 completely covers the cell surface and exhibits oblique symmetry. During growth of *B. stearothermophilus* DSM 2358 on starch medium, three amylases with molecular weights of 58,000, 98,000, and 184,000 were secreted into the culture fluid, but only the high-molecular-weight enzyme was found to be cell associated. Studies of interactions between cell wall components and amylases revealed no affinity of the high-molecular-weight amylase to isolated peptidoglycan. On the other hand, this enzyme was always found to be associated with S-layer self-assembly products or S-layer fragments released during preparation of spheroplasts by treatment of whole cells with lysozyme. The molar ratio of S-layer subunits to the bound amylase was approximately 8:1, which corresponded to one enzyme molecule per four morphological subunits. Immunoblotting experiments with polyclonal antisera against the high-molecular-weight amylase revealed a strong immunological signal in response to the enzyme but no cross-reaction with the S-layer protein or the smaller amylases. Immunogold labeling of whole cells with anti-amylase antiserum showed that the high-molecular-weight amylase is located on the outer face of the S-layer lattice. Because extraction of the amylase was possible without disintegration of the S-layer lattice into its constituent subunits, it can be excluded that the enzyme is incorporated into the crystal lattice and participates in the self-assembly process. Affinity experiments strongly suggest the presence of a specific recognition mechanism between the amylase molecules and S-layer protein domains either exposed on the outermost surface or inside the pores. In summary, results obtained in this study confirmed that the S-layer protein from *B. stearothermophilus* DSM 2358 functions as an adhesion site for a high-molecular-weight amylase.

Crystalline bacterial surface layers (S-layers) can now be considered one of the most common surface structures in prokaryotic cells (for reviews, see references 3, 6–9, 15, 19, 20, 28, and 40–44). S-layer lattices are assemblies of identical subunits showing either oblique (p2), trimeric (p3), square (p4), or hexagonal (p6) symmetry. Depending on the lattice type, one morphological unit consists of two (p2), three (p3), four (p4), or six (p6) identical protein or glycoprotein subunits with molecular weights ranging from 30,000 to 200,000.

Although considerable information about the morphology, chemistry, morphogenesis, and genetics of S-layers has accumulated, relatively few reliable data are available about biological functions (for reviews, see references 6, 10, 17, 21, 30, 38, and 47–51).

Bacillus stearothermophilus strains are aerobic, thermophilic organisms which can produce large amounts of exoenzymes such as proteases and amylases (1, 29). Despite considerable diversity regarding the lattice type, the molecular weight of the S-layer subunits, and the presence of covalently bound carbohydrate residues (26), great similarities could be observed in the molecular-sieving properties of their S-layers. An additional common property appears to be a net neutral charge of the S-layer surface and the pore areas (36, 37). Although it has frequently been suggested that S-layers from members of the family *Bacillaceae* can protect the peptidoglycan from muramidases and the protoplast from proteases (40), in the case of *B. stearothermophilus* strains, no experimental evidence could support this assumption. Detailed permeability studies showed that molecules with molecular weights of up to 40,000 can pass through the pores in the S-layer lattices (37). Pores small enough for rejecting lysozyme have only been detected in strains of *Sporosarcina ureae* (5). For a few *Bacillus* strains, it was demonstrated that lysozyme resistance is caused by a modified peptidoglycan but does not result from smaller pores in their S-layer lattices (34).

Because S-layer-carrying *B. stearothermophilus* strains can produce large amounts of exoproteins with molecular weights above the exclusion limit of their S-layers, the involvement of these lattices in exoprotein secretion has to be examined. In this context, it was suggested that S-layers from members of the family *Bacillaceae* could delineate a kind of periplasmic space in cell envelopes of gram-positive organisms (11, 13, 46).

Binding of exoenzymes to the cell surface has recently been reported for the cellulosome of *Clostridium thermocellum* (12, 32, 33) and for the pullulanase of *Thermoanaerobacterium thermosulfurigenes* (25, 45). Although the nucleotide sequence of the S-layer gene of *T. thermosulfurigenes* has not yet been elucidated, comparison of sequence data between the pullulanase from this organism and the S-layer proteins from different bacterial strains revealed that the enzyme might be able to integrate into the S-layer lattice because of the presence of structurally homologous domains (25). Under conditions in which degradation of the cell envelope, including the S-layer lattice, occurred, attachment sites for the enzyme were lost; consequently it was released into the culture fluid (25).

In our report, a model for attachment of the high-molecular-weight amylase to the S-layer protein of *B. stearothermophilus* DSM 2358 based on affinity studies and immunolabeling techniques is proposed which assigns the S-layer of *B. stearothermophilus* DSM 2358 a new function.

* Corresponding author. Mailing address: Zentrum für Ultrastrukturforschung, Universität für Bodenkultur, Gregor-Mendelstr. 33, A-1180 Vienna, Austria. Phone: 0043 1 47 654 2208. Fax: 0043 1 34 61 76.

MATERIALS AND METHODS

Bacterial strain and growth conditions. *B. stearothermophilus* DSM 2358 was grown in 300-ml shaking flasks on 80 ml of complex medium (4.0 g of peptone, 4.0 g of laboratory Lemco powder, 4.0 g of $(NH_4)_2HPO_4$, 1.0 g of KCl, 0.5 g of $MgSO_4 \cdot 7H_2O$, 1.0 g of soluble starch [Merck] per liter [pH 7.0]) at 50°C for up to 20 h. For inoculation, a bacterial suspension (3 ml) in the late-logarithmic growth phase cultivated on SVIII medium (2) without any carbon source was used. For surveillance of bacterial growth, the pH value was determined and absorption of suspensions (optical density) was measured per hour at 600 nm (Beckmann spectrophotometer, model 25). For immunogold-labeling control experiments, cells were cultivated on SVIII medium (2) containing 0.3% glucose as the sole carbon source.

Determination of amylase activity. Amylase activity of culture fluids and cell pellets was measured according to the method of Bernfeld (4). Protein bands with amylolytic activity were visualized in situ on sodium dodecylsulfate (SDS)-polyacrylamide gels (23) as described by Lacks and Springhorn (22).

Specimen preparation for electron microscopy. Ultrathin sectioning, freeze etching, negative staining, and electron microscopy were performed as previously described (26).

Preparation of cell wall fragments and S-layer self-assembly products and isolation of peptidoglycan. Preparation of cell wall fragments from whole cells was done according to the procedure of Sleytr and Glauert (39), except that whole cells were broken by ultrasonification under conditions described previously (26). Extraction of the plasma membrane with Triton X-100 (Serva; 0.5% in Tris-HCl buffer [pH 7.2]) was done according to the procedure of Sleytr and Glauert (39). Purity of cell wall fragments was checked by SDS-polyacrylamide gel electrophoresis (PAGE) (23) and negative staining.

To produce S-layer self-assembly products, the S-layer protein from cell wall fragments was extracted with guanidinium hydrochloride (GHCl) (5 M GHC1 in 50 mM Tris-HCl buffer [pH 7.2]) for 20 min at 20°C. After centrifugation at 40,000 × *g* for 20 min, the supernatant was dialyzed against distilled water at 4°C for 24 h. Samples were examined by negative staining as previously described (26). S-layer self-assembly products obtained after dialysis were recovered by centrifugation of suspensions at 40,000 × *g* for 20 min. Both sedimented S-layer self-assembly products and clear supernatants containing nonassembled S-layer protein (16) were used for further analysis. Pellets of S-layer self-assembly products were subsequently washed with 50 mM Tris-HCl buffer (pH 7.2), washed once with distilled water, and finally lyophilized. Such washed self-assembly products free of soluble S-layer protein were used for affinity studies. The purity of the reassembled S-layer protein was checked by SDS-PAGE (23).

For isolation of peptidoglycan, cell wall fragments were extracted twice with 5 M GHCl in 50 mM Tris-HCl buffer (pH 7.2) for 20 min at 20°C. Subsequently, the remaining peptidoglycan pellet was washed four times with 50 mM Tris-HCl buffer (pH 7.2), suspended in a small volume of distilled water, and lyophilized.

Permeability studies. Permeability properties of the S-layer lattice with regard to amylases secreted into the culture fluid were determined after depositing native S-layer-carrying cell wall fragments on a microporous support and cross-linking the S-layer protein with glutaraldehyde. The detailed procedure for preparing such S-layer ultrafiltration membranes (SUMs) is described in previous reports (36, 37). For determining the rejection characteristics of SUMs, disks with a diameter of 25 mm were punched out of the membranes and inserted into 10-ml ultrafiltration cells (Amicon, type 8010). The integrity of the active filtration layer, representing a coherent layer of S-layer-carrying cell wall fragments, was checked by using ferritin (M_r, 440,000; molecular size, 12 nm) as a test protein for filtration experiments. For permeability studies, culture supernatants from the stationary growth phase were collected and dialyzed against distilled water at 4°C for 20 h. The dialyzed culture fluid (8 ml) was concentrated on SUMs by a factor of 4 at a pressure of 2×10^5 Pa at 20°C and a stirring speed of 500 rpm. The feed solution, filtrate, and retentate were lyophilized and subjected to SDS-PAGE. Protein bands with amylolytic activity were detected in situ on SDS gels as previously described (22).

Preparation of spheroplasts. For preparation of spheroplasts, cells were cultivated overnight in shaking flasks in 80 ml of complex medium at 50°C. Cells were harvested by centrifugation at the end of logarithmic growth and washed twice with 50 mM Tris-HCl buffer (pH 7.0) at 20°C. Spheroplasts were prepared by suspending cells in 4 ml of Tris-HCl buffer supplemented with 20 mM $MgCl_2 \cdot 6H_2O$ and 7.5% polyethylene glycol (M_r, 6,000; Merck) as osmotic stabilizer. After addition of hen's egg lysozyme (Sigma) to a final concentration of 40 μg/ml, the suspension was incubated at 20°C with gentle agitation until spheroplast formation was completed (usually after 15 min) as judged by phase-contrast microscopy. After centrifugation of spheroplast suspensions (Eppendorf centrifuge 5402) at 3,000 × *g* at 4°C for 5 min, amylase activity in spheroplast pellets and supernatants was determined as previously described (4).

Treatment of whole cells with 2 M GHCl for extraction of the high-molecular-weight amylase. Cells from the stationary growth phase cultivated in 80 ml of complex medium were collected by centrifugation 17 h after inoculation. A suspension (3 ml) of late-logarithmic-growth-phase cells cultivated on SVIII medium without any carbon source was used as the inoculum. Subsequently, the cells were washed twice with 50 mM Tris-HCl buffer (pH 7.2) at 20°C, suspended in 5 ml of GHCl solution (2 M GHCl in 50 mM Tris-HCl buffer [pH 7.2]), and incubated at 4°C for 10 min. After centrifugation of suspensions at 16,000 × *g* at 4°C for 5 min, the amylase activity of the pellets and supernatants was determined as previously described (4). The amylase activity of untreated cells obtained after incubation of cells in 50 mM Tris-HCl buffer (pH 7.2) was taken as a control. For renaturation of the high-molecular-weight amylase, GHCl extracts were dialyzed against a $CaCl_2$ solution (10 mM $CaCl_2$ in distilled water) at 4°C. The amylase activity of the dialyzed suspension was measured as previously described (4). Subsequently, suspensions containing assembled S-layer protein and showing amylase activity were centrifuged at 40,000 × *g* for 20 min at 4°C. The pellet and the supernatant were investigated by SDS-PAGE. Samples of pellets and dialyzed supernatants obtained by incubation of cells in GHCl solution and Tris-HCl buffer were also investigated by SDS-PAGE.

Studies of interactions between amylases and cell wall components. Lyophilized samples of cell wall fragments (5.0 mg), S-layer self-assembly products (2.5 mg), and isolated peptidoglycan (2.5 mg) were incubated with 3 ml of culture supernatant from the stationary growth phase at 50°C for 30 min. After centrifugation of suspensions at 40,000 × *g* at 20°C for 15 min, the amylase activity of the pellets and supernatants was determined as previously described (4). For determination of specific interactions, amylase activity obtained after incubation of cell wall components with 0.02 M potassium phosphate buffer (pH 7.0) was subtracted from that obtained after incubation with culture supernatant. An increase in amylase activity in pellets of cell wall components after incubation in culture supernatants was considered to be specific binding of amylase. Samples were also investigated by SDS-PAGE.

To study the reassociation between amylase and S-layer subunits, 2 mg of lyophilized S-layer self-assemblies were treated with 4 ml of 2.5 M GHCl in 50 mM Tris-HCl buffer (pH 7.2) at 50°C for 15 min. This GHCl concentration does not disrupt the S-layer lattice but releases the S-layer-bound high-molecular-weight amylase. After dialysis of GHCl extracts against distilled water at 4°C for 3 h, S-layer self-assembly products were recovered by centrifugation (40,000 × *g*, 4°C, 15 min) and amylase activity in the pellet and in the supernatant was determined (4). For determination of amylase activity of S-layer self-assembly products, washed and lyophilized material was resuspended in 50 mM Tris-HCl buffer (pH 7.2) at 50°C and aliquots were used for the amylase test (4). To control the release of amylase or S-layer protein after resuspension in buffer, the suspension was centrifuged at 40,000 × *g* for 20 min at 4°C. The clear supernatant was applied to SDS-PAGE and used to determine amylase activity.

Production of antisera against the high-molecular-weight amylase. For production of polyclonal antisera against the high-molecular-weight amylase, cell wall fragments were separated by SDS-PAGE with an acrylamide concentration for the separation gel of 7.5%. After visualization of the amylase band with Serva Blue W stain (Serva), gel slices were excised, fragmented, and lyophilized. The protein content of one amylase band was estimated densitometrically on silver-stained SDS gels with a Hirschmann densitometer (Elscript 400 AT/SM). Antisera were produced in two rabbits by subcutaneous injection of samples, each of which contained 20 μg of high-molecular-weight amylase in 1 ml of a 0.9% NaCl solution. Injections were performed three times at 3-week intervals. At the same time, the immune response was investigated by the immunoblot technique (14). The antisera were collected 4 weeks after the final injection by bleeding of the ear vein. Inactivation of complement in all antisera was achieved by heating at 56°C for 15 min.

SDS-PAGE and immunoblotting. SDS-PAGE was carried out as previously described (23). For most experiments, a gel system with a 4% stacking gel and a 10% separation gel was used.

The immunospecificity of antisera was investigated by the immunoblot procedure (14). Incubation with anti-amylase antisera was carried out at different dilutions of the antisera in 3% bovine serum albumin in Tris-buffered saline at 37°C for at least 2 h. Detection of proteins that bound the anti-amylase antibodies was accomplished by treatment of blots with alkaline phosphatase-conjugated goat anti-rabbit immunoglobulin G (Sigma) at a 1:2,000 dilution for 1 h.

Electron microscopic immunolabeling experiments. Immunogold labeling was carried out with cells from the stationary growth phase which were cultivated on complex medium containing 1.0 g of soluble starch per liter. Furthermore, an immunolabeling control experiment was done with cells from the logarithmic growth phase which were cultivated on SVIII medium (2) with 0.3% glucose when amylase production was inhibited. Cell pellets from a 1-ml cell suspension were incubated with antiserum I at a 1:10 dilution in phosphate-buffered saline (for at least 2 h) at 20°C. Subsequently, washed cells were treated with a concentrated protein A-colloidal gold conjugate (5 nm; Sigma) for 1 h at 20°C. Unbound protein A-colloidal gold conjugate was removed by three cycles of centrifugation in distilled water. Unfixed and unstained cells were immediately applied to Pioloform-filmed carbon-coated copper grids which had been rendered hydrophilic by glow discharge. Preparations were examined in a Philips EM 301 electron microscope operated at 80 kV.

RESULTS

Characterization of the S-layer from *B. stearothermophilus* DSM 2358. As shown by ultrathin sectioning of whole cells, the peptidoglycan-containing layer was completely covered with an additional layer (Fig. 1a) typical for S-layer-carrying organ-

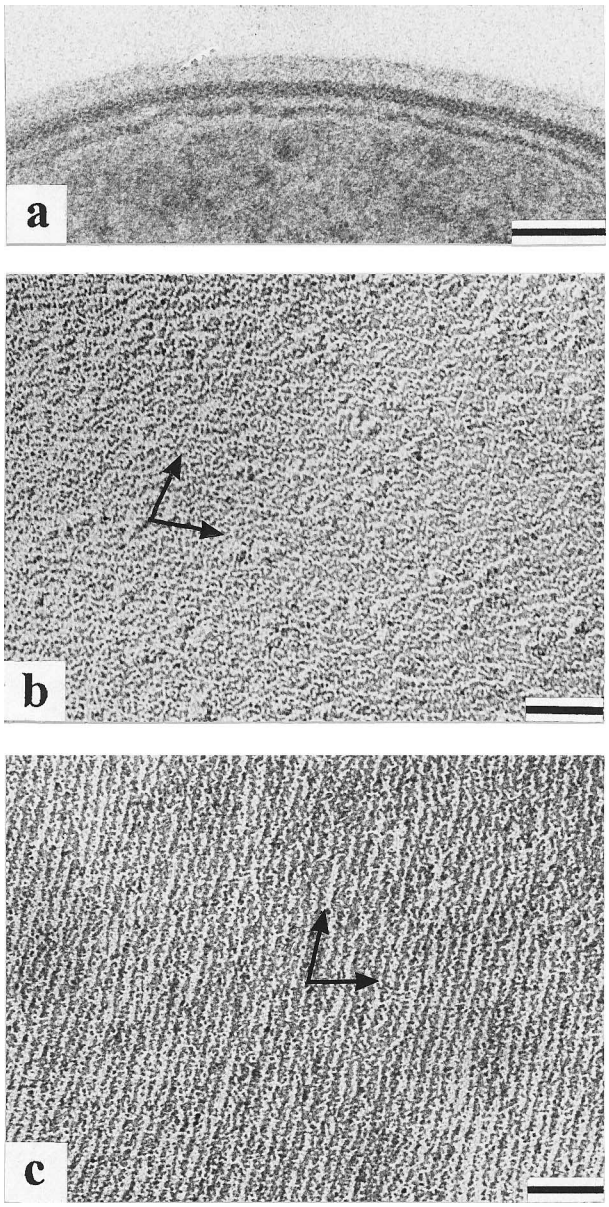

FIG. 1. Electron micrographs from ultrathin-sectioned (a) and freeze-etched (b and c) preparations of whole cells from *B. stearothermophilus* DSM 2358. Cells were investigated before (a and b) and after (c) treatment with 2 M GHCl leading to extraction of the high-molecular-weight amylase. Arrows indicate base vectors. Bars, 50 nm.

isms. In freeze-etched preparations of whole cells (Fig. 1b.), the crystalline structure of the S-layer lattice was not clearly visible and seemed to be covered with amorphous material. After treatment of whole cells with 2 M GHCl (Fig. 1c), a highly ordered S-layer lattice with oblique symmetry which completely covered the cell surface appeared. As shown by SDS-PAGE of SDS extracts from both native cells (Fig. 2B) and cells treated with 2 M GHCl (not shown), the major protein band had an apparent molecular weight of 98,000 and was identified as an S-layer protein.

Growth and amylase production of *B. stearothermophilus* DSM 2358. As determined by SDS-PAGE, protein bands showing amylase activity had molecular weights of either 58,000, 98,000, or 184,000. Secretion of amylases into the culture fluid started already in the early logarithmic growth phase, 3 to 4 h after inoculation (Fig. 2A). Five hours after inoculation, the high-molecular-weight amylase could already be detected in the cell pellet (Fig. 2B) but was not present in the culture supernatant, where it appeared 8 h after inoculation (Fig. 2C). The high-molecular-weight enzyme was the only one found to be associated with the cell pellet, whereas the smaller enzymes could only be detected in the culture fluid (Fig. 2B and C).

Growth of *B. stearothermophilus* DSM 2358 on SVIII medium containing 0.3% glucose as the sole carbon source completely inhibited amylase production (data not shown).

Preparation of cell wall fragments and S-layer self-assembly products. As shown by SDS-PAGE, the high-molecular-weight amylase remained associated with cell wall fragments even after ultrasonification during cell wall preparation and extraction of the plasma membrane with Triton X-100 (Fig. 3a and b). When SDS-PAGE patterns of cell wall fragments were evaluated by densitometry, the molar ratio between S-layer subunits and amylase molecules was estimated to be in the range of 8:1. SDS-PAGE patterns further revealed that it was not possible to separate the high-molecular-weight enzyme from S-layer protein by 5 M GHCl extraction, which is required for completely disrupting the bonds acting in the S-layer lattice. The enzyme was always found to be associated with S-layer self-assembly products formed during removal of GHCl by dialysis (Fig. 3c and d). After sedimentation of S-layer self-assembly products by centrifugation, both soluble S-layer protein representing monomers and oligomers (16) and the high-molecular-weight amylase were detected in supernatants (data not shown). By negative staining, it could be demonstrated that removal of the hydrogen bond-breaking agent by dialysis yielded sheetlike self-assembly products which did not exhibit a distinct lattice structure (data not shown).

Permeability studies. Permeability studies with amylases secreted in the culture fluid of *B. stearothermophilus* DSM 2358 were carried out on SUMs. By using test proteins with well-defined molecular weights, it was demonstrated that the exclusion limit of S-layer lattices from *B. stearothermophilus* strains is in the range of M_r of ~40,000 (36, 37). As revealed by SDS-PAGE, all amylases produced by *B. stearothermophilus* DSM 2358 were rejected by the pores in the S-layer lattice when dialyzed culture fluid was used for ultrafiltration experiments (Fig. 4). These results indicated that all the three amylases (M_rs of 58,000, 98,000, and 184,000) cannot pass through the pores of the S-layer lattice once they have folded into their final conformation.

Extraction of the high-molecular-weight amylase from whole cells with 2 M GHCl. Treatment of whole cells of *B. stearothermophilus* with 2 M GHCl was done for extraction of the high-molecular-weight amylase under conditions in which the S-layer lattice did not disintegrate. This procedure led to solubilization of at least 80% of the high-molecular-weight amylase (M_r of 184,000), whereas only less than 20% of S-layer protein was detected in the GHCl extract. In comparison, after incubation of cells with 50 mM Tris-HCl buffer, only up to 10% of the original amylase activity was released into the supernatant.

The structural integrity of the peptidoglycan-containing layer and the plasma membrane after extraction with 2 M GHCl was ascertained by ultrathin sectioning of whole cells (data not shown). These results strongly indicated that amylase which could not be extracted with 2 M GHCl is located in the intracellular space of whole bacterial cells. This was confirmed by ultrasonic disruption of whole cells, by which less than 10%

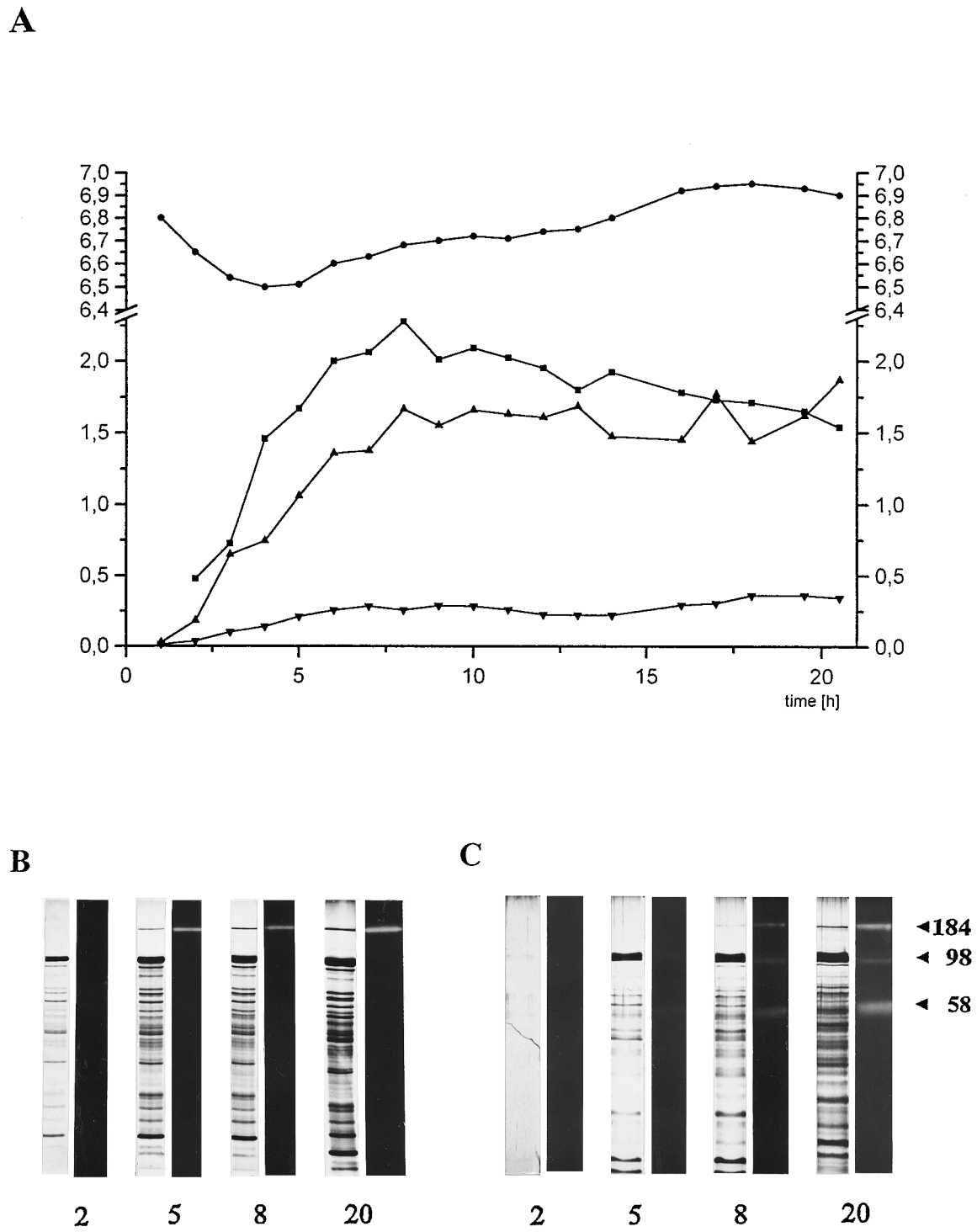

FIG. 2. Growth of *B. stearothermophilus* DSM 2358 in batch culture (A) and detection of amylase in cell pellets (B) and culture supernatants (C) 2, 5, 8, and 20 h after inoculation. Protein bands were visualized by silver staining; bands with amylolytic activity could be detected by applying iodine-starch reagent to SDS gels. Values to the right of panel C are molecular weights (in thousands). ■, optical density at 600 nm; ●, pH; ▲, amylase activity in culture supernatant; ▼, cell-bound amylase activity.

of total amylase activity was detected in the supernatant containing the cytoplasma and plasma membrane fragments.

After removal of GHCl by dialysis, the entire amylase activity was detected in the pellet consisting of reassembled S-layer protein, indicating that the enzyme has affinity to the S-layer protein.

Furthermore, freeze-etched preparations of cells washed with 50 mM Tris-HCl buffer (pH 7.2) and cells treated with 2

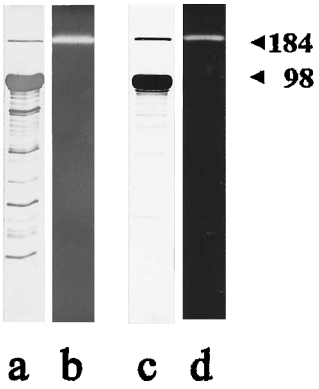

FIG. 3. SDS-PAGE patterns of cell wall fragments (a and b) and sedimented S-layer self-assembly products (c and d) from *B. stearothermophilus* DSM 2358. Lanes a and c, silver staining; lanes b and d, in situ detection of amylase. The high-molecular-weight amylase remained associated with the S-layer protein. Values to the right are molecular weights (in thousands).

M GHCl revealed remarkable differences in their surface structure. On washed cells, the S-layer lattice was always covered with a granular structure (Fig. 1b), while cells treated with 2 M GHCl displayed an undistorted, highly ordered lattice structure (Fig. 1c). As estimated from densitometric evaluation, the molar ratio between S-layer subunits and amylase was 8:1. Because the molecular weight of one amylase molecule is twice as large as that of the S-layer subunits, one enzyme molecule could cover one morphological subunit consisting of two identical S-layer subunits. Assuming a uniform distribution of the high-molecular-weight amylase over the entire cell surface, every fourth morphological unit will be covered with one enzyme molecule, which could be responsible for the loss of the regular appearance of the S-layer lattice in freeze-etched preparations. Because the high-molecular-weight amylase and the S-layer protein represented the major protein bands when dialyzed 2 M GHCl extracts were subjected to SDS-PAGE (not shown), the knoblike structures on the cell surface most likely represented amylase molecules.

Formation of spheroplasts. During degradation of the peptidoglycan-containing layer with lysozyme in the presence of polyethylene glycol, no significant release of high-molecular-weight amylase could be detected. The entire amylase activity was found to be associated with the pellet, which consisted of spheroplasts and S-layer fragments (Fig. 5). In comparison with untreated cell pellets, an increase in amylase activity of approximately 40% could be detected in the spheroplast pellet after degradation of the peptidoglycan-containing layer. These results provided strong evidence that the enzyme is not incorporated into the peptidoglycan layer.

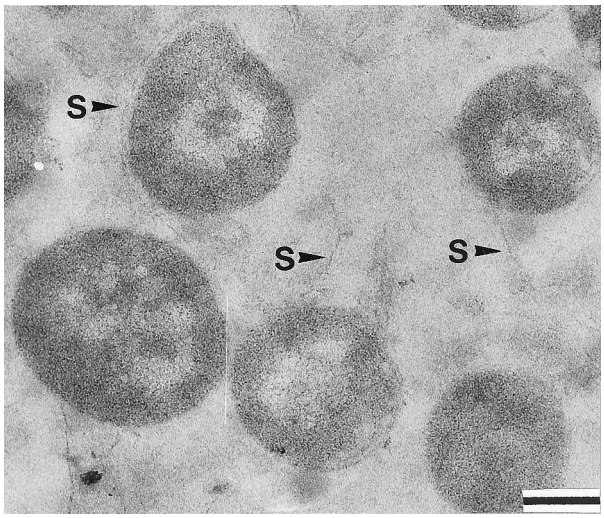

FIG. 5. Ultrathin sections confirming the integrity of spheroplasts from *B. stearothermophilus* DSM 2358. S-layer fragments (S) were also detected in pellets of spheroplasts. Bar, 500 nm.

Studies of interactions between amylases and cell wall components (including peptidoglycan-containing sacculi and S-layer). In the present study, the affinity of cell wall components to amylases secreted into the culture fluid was investigated. Because the high-molecular-weight amylase remained associated with cell wall fragments and S-layer self-assembly products, blanks of amylase activity were determined after incubation of cell wall components in 0.2 M potassium phosphate buffer (pH 7.0). The high-molecular-weight amylase showed affinity to S-layer-carrying cell wall fragments, in which only the outer face of the S-layer lattice was accessible, and to S-layer self-assembly products (Table 1 and Fig. 6a to d) but showed no affinity to isolated peptidoglycan (Table 1 and Fig. 6e to h). The small increase in amylolytic activity of peptidoglycan was due to reattachment of S-layer protein (16) always present in the culture fluid, which could obviously function as an adhesion site for the high-molecular-weight amylase (Fig. 6e to h).

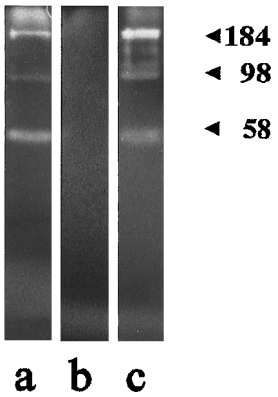

FIG. 4. SDS-PAGE patterns from ultrafiltration experiments with dialyzed culture fluids from *B. stearothermophilus* DSM 2358. Lanes: a, feed solution; b, filtrate; c, retentate. Lanes show results from in situ detection of amylases.

TABLE 1. Interactions between amylases and cell wall components of *B. stearothermophilus* DSM 2358[a]

Component(s)	Amylase activity after incubation of component in:		Binding of amylase
	Culture supernatant	Phosphate buffer	
S-layer protein	0.480	0.275	0.205
Cell wall fragments	1.226	1.070	0.156
Peptidoglycan	0.081	0.002	0.079

[a] For determination of specific interactions, amylase activity determined after incubation of cell wall components in 0.02 M potassium phosphate buffer (pH 7.0) was subtracted from that obtained after incubation with culture supernatant and centrifugation. The increase in amylase activity after incubation of isolated peptidoglycan in culture supernatant was due to reattachment of S-layer protein associated with amylase present in the culture fluid. Amylase activity was determined as previously described (4).

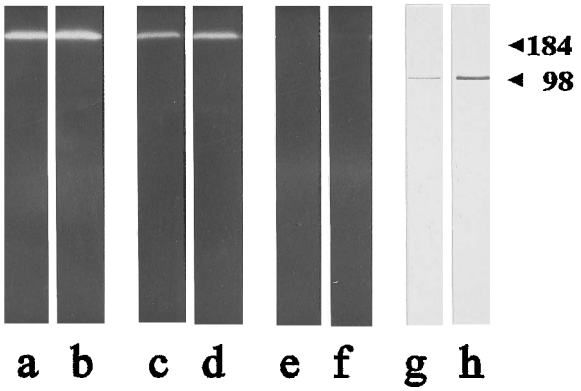

FIG. 6. SDS-PAGE patterns demonstrating affinity of the high-molecular-weight amylase to cell wall fragments (a and b), S-layer self-assembly products (c and d), and isolated peptidoglycan (e, f, g, and h) of *B. stearothermophilus* DSM 2358. Lanes a, c, e, and g, samples incubated in buffer; lanes b, d, f, and h, samples incubated in culture supernatant. Lanes a to f show in situ detection of amylase results, and lanes g and h show silver staining results. Note the reattachment of S-layer protein to isolated peptidoglycan. Values to the right are molecular weights (in thousands).

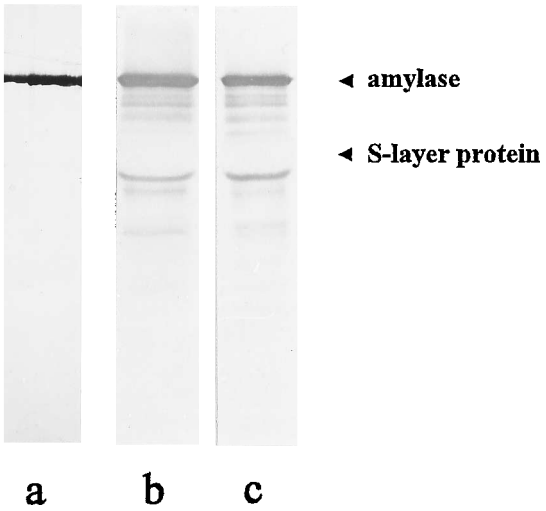

FIG. 7. SDS-PAGE patterns (a) confirming the purity of the high-molecular-weight amylase used for production of polyclonal rabbit antiserum. Lanes b and c, immunoreactivity of whole cells (b) and cell wall fragments (c) of *B. stearothermophilus* DSM 2358 with antiserum I at a dilution of 1:5,000 against the high-molecular-weight amylase. The positions of the high-molecular-weight amylase and S-layer protein are marked.

Furthermore, studies of the reassociation of the S-layer lattice with the high-molecular-weight amylase after its extraction with 2.5 M GHCl were carried out. This GHCl concentration was chosen because it disrupts the bonds between the amylase and S-layer protein but not those between the S-layer subunits.

After treatment of S-layer self-assembly products with 2.5 M GHCl and subsequent dialysis, even 110% of amylase activity could be detected in the self-assembly fraction. No amylase activity or S-layer protein was left in the supernatant. Because removal of 2.5 M GHCl led to a complete reassociation of the enzyme with the S-layer lattice, a specific recognition mechanism between the S-layer subunits arranged in the crystal lattice and the at least partly unfolded enzyme molecules seems to exist.

Immunoblotting and localization of the high-molecular-weight amylase by immunogold-labeling techniques. The purity of the excised amylase bands used for immunization was confirmed by SDS-PAGE (Fig. 7a). Amylase fractions consisted of a single protein band and showed no contamination with other proteins.

The immunospecificity of the anti-amylase antisera was investigated by immunoblotting (Fig. 7b and c). In addition to the high-molecular-weight amylase, which gave a strong immunological signal, a few plasma proteins showed a weak cross-reaction with antisera I and II at a dilution of 1:5,000. On the contrary, neither the other amylases nor the S-layer protein cross-reacted with the antisera. The application of preimmune serum showed no nonspecific labeling. When cells were grown in the presence of glucose as a carbon source where amylase production was inhibited, no high-molecular-weight amylase labeling could be detected on immunoblots.

The high-molecular-weight amylase was localized at the cell surface by immunolabeling experiments (Fig. 8). Electron micrographs of immunogold-labeled cells revealed that cells had collapsed during drying on the grid. The dark central region represented the shrunken protoplast which retracted from the cell wall. The surface of cells grown on starch-medium was densely labeled with antibodies against the high-molecular-weight amylase (Fig. 8a). In comparison, the immunolabeling procedure led to a significantly lower marker density on cells grown in the presence of high glucose concentrations where amylase production was inhibited (Fig. 8b).

DISCUSSION

To investigate the function of the S-layer lattice in *Bacillus* species with regard to exoprotein secretion, *B. stearothermophilus* DSM 2358 was used as a model system in this study. This organism is completely covered with an oblique S-layer lattice and was shown to secrete three amylases with molecular weights of 58,000, 98,000, and 184,000 into the culture fluid.

Permeability studies applying the SUM technique (36, 37) and using culture supernatants for ultrafiltration experiments showed that the S-layer lattice completely rejected the enzymes once they had assumed their final three-dimensional structure. Amylase secretion of this organism already started in the logarithmic growth phase, which is different from observations reported for most *Bacillus* strains, in which exoenzyme secretion starts in the stationary growth phase parallel to degradation of cell wall components in the course of increased autolytic activity (1, 29). Although little information is available, the most common mechanism suggested for release of exoenzymes is an increase in permeability of the cell wall matrix induced by autolytic degradation (1, 29).

As derived from permeability studies, in the case of *B. stearothermophilus* DSM 2358, passage of amylases through the pores in the S-layer lattice of actively growing cells is only possible for enzyme molecules prefolded into smaller domains. After passage through the cell wall, complete folding of enzymes into their final three-dimensional structure will occur either on the cell surface or after release into the culture fluid.

For many proteins that have accumulated in a kind of periplasmic space in the cell envelopes of gram-positive organisms, peptidoglycan strands or secondary cell wall polymers could function as spacers, thereby preventing complete folding of proteins into the final three-dimensional conformation (16, 18). Because amylase secretion occurs in the logarithmic growth phase, in which the cell surface is extended, enzyme secretion is also possible, in principle, at sites of peptidoglycan and S-layer lattice growth.

Several experiments performed in this study confirmed that the high-molecular-weight amylase has affinity to the S-layer

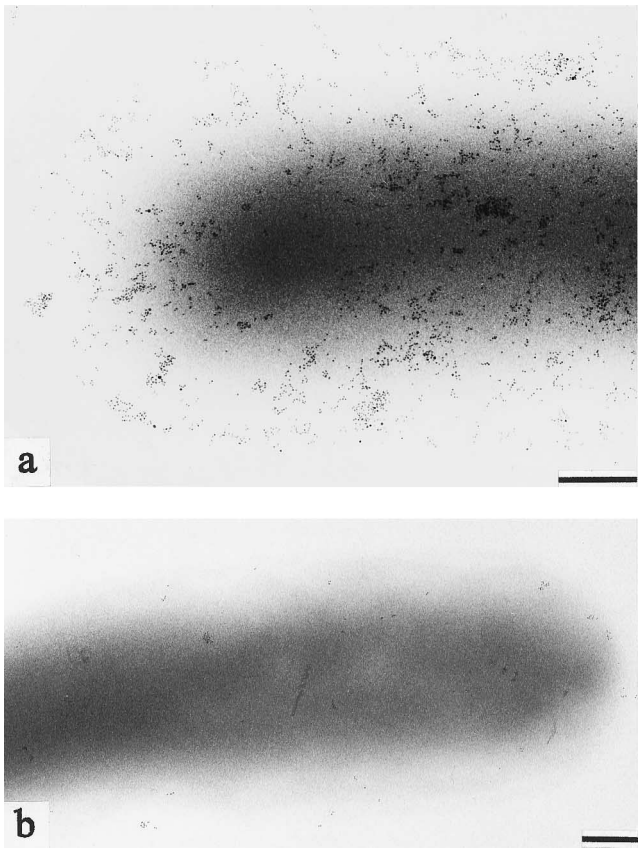

FIG. 8. Protein A-colloidal gold labeling with a polyclonal rabbit antiserum raised against the high-molecular-weight amylase on whole cells from *B. stearothermophilus* DSM 2358. (a) Immunogold labeling of the high-molecular-weight amylase on cells grown on starch medium. (b) Negative control experiment with cells grown in the presence of a high glucose concentration in which amylase production is inhibited. Bars, 200 nm.

protein but not to peptidoglycan. Furthermore, from experimental data, it can be excluded that the amylase associated with the S-layer protein is integrated into the cytoplasmic membrane in native cells. Cells grown on complex medium and used for freeze-etching revealed a granular structure on the surface of the S-layer lattice which could completely be removed with 2 M GHCl. Because after dialysis of GHCl extracts 80% of the original amylase activity was detected in this fraction, we suggest that the particulate material on the S-layer surface represented amylase molecules. The molar ratio of S-layer subunits to amylase molecules was 8:1, which means that—assuming there is a uniform distribution of enzyme molecules on the cell surface—every fourth morphological unit is covered with an amylase molecule. This could be responsible for the loss of the regular appearance of the oblique S-layer lattice in freeze-etched preparations. The surface location of the high-molecular-weight amylase was finally confirmed by immunogold labeling of whole cells. Although it was shown that at least a major portion of the amylase is located on the outer face of the S-layer lattice, the question arises as to how the enzyme is associated with the S-layer protein. Generally, three possibilities exist: (i) adhesion of the amylase to the S-layer surface; (ii) incorporation of the enzyme into the S-layer lattice, which would imply that the enzyme is involved in the self-assembly process; and (iii) binding of the enzyme to S-layer protein domains exposed inside the pores.

Because extraction of a major portion of amylase from the cell surface with 2 M GHCl did not require disintegration of the S-layer lattice, the possibility that the high-molecular-weight enzyme is integrated into the S-layer lattice can be excluded. S-layer-integrated amylase domains would probably interfere with the S-layer self-assembly process, which was not observed in this study. Experiments with different GHCl concentrations also supported the notion that bonds between amylase molecules and S-layer subunits are much weaker than those between S-layer subunits required for the integrity of the S-layer lattice. Furthermore, if the high-molecular-weight amylase molecules participated in the self-assembly process of the S-layer, they would require the capability for exactly replacing one or two S-layer subunits. Binding of the amylase is therefore suggested to occur to protein domains either located at the surface of the crystal lattice or exposed inside the pores.

As observed by immunoblotting, polyclonal antibodies raised against the high-molecular-weight amylase did not cross-react with S-layer protein or the other two amylases. These results indicate that the amylase and the S-layer protein do not possess structurally homologous domains. The existence of structurally homologous domains to S-layer proteins which were suggested to be involved in the recognition mechanism was described for the pullulanase of *T. thermosulfurigenes* (25), the cellulosome of *C. thermocellum* (12, 32, 33), and an endoxylanase of *Thermoanaerobacter saccharolyticum* (24).

Computer image reconstructions of S-layers from several thermophilic *Bacillus* strains revealed at least two types of pores differing in size and morphology (27, 31, 35). As discussed in a previous paper, the different pores in the lattices might be related to specific functions (36). One type of pore could be necessary for guaranteeing unhindered passage of nutrients, whereas the other pore could play an important role in exoenzyme secretion. Exoproteins are translocated via their N terminus, which is the first part of the protein molecule that can independently prefold into domains and will appear on the cell surface. Attachment of enzymes to S-layer proteins inside the pores would most likely occur with their C-terminal region.

In the present study, we confirmed that the S-layer lattices from *B. stearothermophilus* DSM 2358 function as adhesion sites for the cells' own exoproteins. Considering that the S-layer lattice represents the first contact region and has most likely evolved as a consequence of interactions between the living cell and its environment, other biological functions cannot be excluded. Location of the amylase at the cell surface is advantageous because the enzyme can function as a mediator between the living cell and a high-molecular-weight substrate (32). The S-layer lattice as a highly porous ultrafiltration membrane guarantees rapid diffusion for degradation products with molecular weights up to 30,000 to 40,000 into the cell wall, where they can further be hydrolyzed by the smaller amylases located in a kind of periplasmic space delineated by the S-layer lattice (11, 36).

ACKNOWLEDGMENTS

This work was supported by the Fonds zur Förderung der Wissenschaftlichen Forschung in Österreich (project S72/02) and by the Österreichisches Bundesministerium für Wissenschaft und Forschung.

We thank Andrea Scheberl for excellent technical assistance.

REFERENCES

1. **Archibald, R.** 1989. The *Bacillus* cell envelope, p. 217–254. *In* C. R. Harwood (ed.), *Bacillus*, biotechnology handbook 2. Plenum Press, New York.
2. **Bartelmus, W., and F. Perschak.** 1957. Schnellmethode zur Keimzahlbestimmung in der Zuckerindustrie. Z. Zuckerind. **7:**276–281.
3. **Baumeister, W., and H. Engelhardt.** 1987. Three-dimensional structure of bacterial surface layers, p. 109–154. *In* J. R. Harris and R. W. Horne (ed.),

Electron microscopy of proteins, vol. 6. Membraneous structures. Academic Press Ltd., London.
4. **Bernfeld, P.** 1955. Amylases α and β. Methods Enzymol. **1:**149–158.
5. **Beveridge, T. J.** 1979. Surface arrays on the wall of *Sporosarcina ureae*. J. Bacteriol. **139:**1039–1048.
6. **Beveridge, T. J.** 1981. Ultrastructure, chemistry and function of the bacterial cell wall. Int. Rev. Cytol. **72:**229–317.
7. **Beveridge, T. J.** 1994. Bacterial S-layers. Curr. Opin. Struct. Biol. **4:**204–212.
8. **Beveridge, T. J., and L. L. Graham.** 1991. Surface layers of bacteria. Microbiol. Rev. **55:**684–705.
9. **Beveridge, T. J., and S. F. Koval (ed.).** 1993. Advances in bacterial paracrystalline surface layers. Plenum Press, New York.
10. **Blaser, M. J., and E. C. Gotschlich.** 1990. Surface array protein of *Campylobacter fetus*: cloning and gene structure. J. Biol. Chem. **265:**14529–14535.
11. **Breitwieser, A., K. Gruber, and U. B. Sleytr.** 1992. Evidence for an S-layer pool in the peptidoglycan of *Bacillus stearothermophilus*. J. Bacteriol. **174:** 8008–8015.
12. **Fujino, T., P. Béguin, and J.-P. Aubert.** 1993. Organization of a *Clostridium thermocellum* gene cluster encoding the cellulosomal scaffolding protein CipA and a protein possibly involved in attachment of the cellulosome to the cell surface. J. Bacteriol. **175:**1891–1899.
13. **Graham, L. L., T. J. Beveridge, and N. Nanninga.** 1991. Periplasmic space and the concept of periplasm. Trends Biochem. Sci. **16:**328–329.
14. **Harlow, E., and D. Lane.** 1988. Antibodies: a laboratory manual. Cold Spring Harbor Laboratory, Cold Spring Harbor, N.Y.
15. **Hovmöller, S., A. Sjörgen, and D. N. Wang.** 1988. The structure of crystalline bacterial cell surface layers. Prog. Biophys. Mol. Biol. **51:**131–163.
16. **Jaenicke, R., R. Welsch, M. Sára, and U. B. Sleytr.** 1985. Stability and self-assembly of the S-layer protein of the cell wall of *Bacillus stearothermophilus*. Biol. Chem. Hoppe-Seyler **366:**663–670.
17. **Kay, W. W., J. C. Thornton, and R. A. Garduno.** 1993. Structure-function aspects of the *Aeromonas salmonicida* S-layer, p. 151–158. *In* T. J. Beveridge and S. F. Koval (ed.), Advances in bacterial paracrystalline surface layers. Plenum Publishing Corp., New York.
18. **Kern, G., N. Schülke, F. X. Schmid, and R. Jaenicke.** 1992. Stability, quaternary structure, and folding of internal, external, and core-glycosylated invertase from yeast. Protein Sci. **1:**120–131.
19. **König, H.** 1988. Archaeobacterial cell envelopes. Can. J. Microbiol. **33:**395–406.
20. **Koval, S. F.** 1988. Paracrystalline protein surface arrays on bacteria. Can. J. Microbiol. **33:**407–414.
21. **Koval, S. F.** 1993. Predation on bacteria possessing S-layers, p. 85–92. *In* T. J. Beveridge and S. F. Koval (ed.), Advances in bacterial paracrystalline surface layers. Plenum Publishing Corp., New York.
22. **Lacks, S. A., and S. S. Springhorn.** 1980. Renaturation of enzymes after polyacrylamide gel electrophoresis in the presence of sodium dodecyl sulfate. J. Biol. Chem. **255:**7467–7473.
23. **Laemmli, U. K.** 1970. Cleavage of structural proteins during the assembly of the head of bacteriophage T4. Nature (London) **227:**680–685.
24. **Lupas, A., H. Engelhardt, J. Peters, U. Santarius, S. Volker, and W. Baumeister.** 1994. Domain structure of the *Acetogenium kivui* surface layer revealed by electron crystallography and sequence analysis. J. Bacteriol. **176:**1224–1233.
25. **Matuschek, M., G. Burchhardt, K. Sahm, and H. Bahl.** 1994. Pullulanase of *Thermoanaerobacterium thermosulfurigenes* EM1 (*Clostridium thermosulfurogenes*): molecular analysis of the gene, composite structure of the enzyme, and a common model for its attachment to the cell surface. J. Bacteriol. **176:**3295–3302.
26. **Messner, P., F. Hollaus, and U. B. Sleytr.** 1984. Paracrystalline cell wall surface layers of different *Bacillus stearothermophilus* strains. Int. J. Syst. Bacteriol. **34:**202–210.
27. **Messner, P., D. Pum, and U. B. Sleytr.** 1986. Characterization of the ultrastructure and the self-assembly of the surface layer of *Bacillus stearothermophilus* strain NRS 2004/3a. J. Ultrastruct. Mol. Struct. Res. **97:**73–88.
28. **Messner, P., and U. B. Sleytr.** 1992. Crystalline bacterial cell surface layers. Adv. Microb. Physiol. **33:**213–275.
29. **Priest, F. G.** 1981. Products and applications, p. 293–320. *In* C. R. Harwood (ed.), *Bacillus*, biotechnology handbook 2. Plenum Press, New York.
30. **Pum, D., P. Messner, and U. B. Sleytr.** 1991. Role of the S layer in morphogenesis and cell division of the archaebacterium *Methanocorpusculum sinense*. J. Bacteriol. **173:**6865–6873.
31. **Pum, D., M. Sára, and U. B. Sleytr.** 1989. Structure, surface charge, and self-assembly of the S-layer lattice from *Bacillus coagulans* E38-66. J. Bacteriol. **171:**5296–5303.
32. **Salamitou, S., M. Lemaire, T. Fujino, H. Ohayon, P. Gounon, P. Béguin, and J.-P. Aubert.** 1994. Subcellular localization of *Clostridium thermocellum* ORF3p, a protein carrying a receptor for the docking sequence borne by the catalytic components of the cellulosome. J. Bacteriol. **176:**2828–2834.
33. **Salamitou, S., O. Raynaud, M. Lemaire, M. Coughlan, P. Béguin, and J.-P. Aubert.** 1994. Recognition specificity of the duplicated segments present in *Clostridium thermocellum* endoglucanase CelD and in cellulosome-integrating protein CipA. J. Bacteriol. **176:**2822–2827.
34. **Sára, M., K. Moser-Thier, U. Kainz, and U. B. Sleytr.** 1990. Characterization of S-layers from mesophilic Bacillaceae and studies on their protective role towards muramidases. Arch. Microbiol. **153:**209–214.
35. **Sára, M., D. Pum, S. Küpcü, P. Messner, and U. B. Sleytr.** 1994. Isolation of two physiologically induced variant strains of *Bacillus stearothermophilus* NRS 2004/3a and characterization of their S-layer lattices. J. Bacteriol. **176:**848–860.
36. **Sára, M., D. Pum, and U. B. Sleytr.** 1992. Permeability and charge-dependent adsorption properties of the S-layer lattice from *Bacillus coagulans* E38-66. J. Bacteriol. **174:**3487–3493.
37. **Sára, M., and U. B. Sleytr.** 1987. Production and characteristics of ultrafiltration membranes with uniform pores from two dimensional arrays of proteins. J. Membr. Sci. **33:**27–49.
38. **Schultze-Lam, S., and T. J. Beveridge.** Ultrastructural and chemical characterization of a cyanobacterial S-layer involved in fine-grain mineral formation, p. 67–75. *In* T. J. Beveridge and S. F. Koval (ed.), Advances in bacterial paracrystalline surface layers. Plenum Publishing Corp., New York.
39. **Sleytr, U. B., and A. M. Glauert.** 1975. Self-assembly of the hexagonally and tetragonally arranged subunits of bacterial surface layers and their reattachment to cell walls. J. Ultrastruct. Res. **55:**360–377.
40. **Sleytr, U. B., and P. Messner.** 1983. Crystalline surface layers on bacteria. Annu. Rev. Microbiol. **37:**311–339.
41. **Sleytr, U. B., and P. Messner.** 1988. Crystalline surface layers in procaryotes. J. Bacteriol. **170:**2891–2897.
42. **Sleytr, U. B., P. Messner, D. Pum, and M. Sára (ed.).** 1988. Crystalline bacterial cell surface layers. Springer, Berlin.
43. **Sleytr, U. B., P. Messner, D. Pum, and M. Sára.** 1993. Crystalline bacterial cell surface layers. Mol. Microbiol. **10:**911–916.
44. **Smit, J.** 1986. Protein surface layers of bacteria, p. 343–376. *In* M. Inouye (ed.), Bacterial outer membranes as model systems. John Wiley & Sons, Inc., New York.
45. **Specka, U., A. Spreinat, G. Antranikian, and F. Mayer.** 1991. Immunocytochemical identification and localization of active and inactive α-amylase and pullulanase in cells of *Clostridium thermosulfurogenes* EM1. Appl. Environ. Microbiol. **57:**1062–1069.
46. **Sturm, E., E. Egelseer, M. Sára, and U. B. Sleytr.** 1993. Can S-layers of Bacillaceae control the release of their own exoproteins? p. 297–302. *In* T. J. Beveridge and S. F. Koval (ed.), Advances in bacterial paracrystalline surface layers. Plenum Publishing Corp., New York.
47. **Trust, T. J.** 1993. Molecular, structural and functional properties of *Aeromonas* S-layers, p. 159–171. *In* T. J. Beveridge and S. F. Koval (ed.), Advances in bacterial paracrystalline surface layers. Plenum Publishing Corp., New York.
48. **Tummuru, M. K. R., and M. J. Blaser.** 1992. Characterization of the *Campylobacter fetus sapA* promoter: evidence that the *sapA* promoter is deleted in spontaneous mutant strains. J. Bacteriol. **174:**5916–5922.
49. **Tummuru, M. K. R., and M. J. Blaser.** 1993. Rearrangement of *sapA* homologs with conserved and variable regions in *Campylobacter fetus*. Proc. Natl. Acad. Sci. USA **90:**7265–7269.
50. **Wang, E., M. M. Garcia, M. S. Blake, Z. Pei, and M. J. Blaser.** 1993. Shift in S-layer protein expression responsible for antigenic variation in *Campylobacter fetus*. J. Bacteriol. **175:**4979–4984.
51. **Wildhaber, J., and W. Baumeister.** 1987. The cell envelope of *Thermoproteus tenax*. Three-dimensional structure of the surface layer and its role in shape maintenance. EMBO J. **6:**1475–1480.